IEEE Access
Multidisciplinary | Rapid Review | Open Access Journal

Date of publication xxxx 00, 0000, date of current version xxxx 00, 0000.

Digital Object Identifier 10.1109/ACCESS.2017.Doi Number

Damping Torque Analysis of VSC-HVDC Supplementary Damping Controller for Small-signal Stability

TAO ZHOU[1,2], ZHONG CHEN[2,3], BIXING REN[4], SIQI BU[5], (Senior Member, IEEE), PUYU WANG[1], (Member, IEEE)

[1]School of Automation, Nanjing University of Science and Technology, Nanjing 210094, China
[2]Jiangsu Key Laboratory of Smart Grid Technology and Equipment, Nanjing 210096, China
[3]School of Electrical Engineering, Southeast University, Nanjing 210096, China
[4]State Grid Jiangsu Electric Power Company Ltd., Research Institute, Nanjing 211103, China
[5]Department of Electrical Engineering, The Hong Kong Polytechnic University, Hong Kong

Corresponding author: Tao Zhou (zhoutaonjust@njust.edu.cn).

This work was supported in part by the National Key Research and Development Program under Grant 2016YFB0900602, in part by the Jiangsu Key Laboratory of Smart Grid Technology and Equipment.

ABSTRACT In order to improve the small-signal stability of AC/DC hybrid systems containing voltage-source converter based high-voltage direct current (VSC-HVDC), this paper extends damping torque analysis (DTA) theory to VSC-HVDC supplementary damping controller to analyze its dynamic impacts and inhibit oscillations. Firstly, this paper presents the mechanism and procedure of VSC supplementary damping controller and establishes the linearized model of AC/DC system with damping controllers. On this basis, the DTA theory of VSC supplementary damping controller and the equation of damping torque index (DTI) are derived. The theory can be applied to the design of the damping controller including the selection of installation location and channel as well as the parameter tuning. Finally, case studies are carried out in two AC/DC hybrid systems containing VSC-HVDC. The simulation results verify the correctness and feasibility of DTI analysis. VSC damping controllers designed by the proposed method can effectively suppress oscillations and improve the dynamic stability of the AC/DC system.

INDEX TERMS VSC-HVDC; supplementary damping controller; damping torque analysis (DTA); small-signal stability; AC/DC system

I. INTRODUCTION

VSC-HVDC has been widely developed and applied for its unique advantages including no communication failure, less voltage harmonics, independent separated control of active and reactive powers and so on [1-3]. VSC-HVDC brings about new challenges to the security and operation of power grids. According to [4, 5], when connected with weak AC systems and adopting vector current control (VCC), the dynamics of phase-locked loop (PLL) may lead to instability of the whole system. The interaction between VSC control and other controllers may cripple system damping which is harmful to system stability [6]. In addition, some investigations have shown VSC-HVDC may trigger sub-synchronous oscillations because of open-loop modal coupling [7, 8]. Therefore, it is necessary to install supplementary damping controllers to inhibit oscillations and guarantee the stable operation of AC/DC system with VSC-HVDC.

Research and design of VSC supplementary damping controller have been extensively investigated in recent years. VSC supplementary damping controller can enhance the decoupled power control of VSC stations so as to improve system dynamics [9, 10]. In [11], a centralized multiple input multiple output (MIMO) supplementary controller is devised based on linear matrix inequality (LMI) based on regional pole configuration and homotopy transformation. The designed robust controllers which can coordinate active and reactive power have many advantages such as low order, no cross-coupling, stronger robustness and good performance of suppressing low frequency oscillation. In order to damp critical modes, [12] proposes a robust probabilistic control structure which investigates the know variation of operation

This article has been accepted for publication in a future issue of this journal, but has not been fully edited. Content may change prior to final publication. Citation information: DOI 10.1109/ACCESS.2020.3036495, IEEE Access

condition to recognize the probabilistic locations of these eigenvalues. Thus, the modal linear quadratic Gaussian (MLQG) controller is designed based on a few probabilistic modes. In [13], supplementary damping controller is designed based entire-dimension state feedback space. The controller adjusts the active power of VSC according to the frequency fluctuation so as to damp oscillations. [14] implements a novel power oscillation damping controller structure and proposes a robust probabilistic method to evaluate its performance. A model predictive controller which can handle the injection powers of DC transmission lines to damp oscillations is proposed in [15]. The controller analyzes the constraints and expected future performance of AC/DC system and takes them into the design procedure. In [16], it shows that with proper control design, virtual synchronous machines (VSMs) can provide considerable positive damping torque to effectively damp low frequency oscillations in power grids. Besides, it is found that the internal angle and frequency of the VSC stations can be used to damping oscillations as they also strongly couple with generator angles and speeds which provides new ideas for oscillation suppression of the AC/DC system. These investigations mainly focus on the innovation of controller structure based on control theory to inhibit oscillations in AC/DC system containing VSC-HVDC.

Damping torque analysis is an important and efficient method for small-signal stability analysis, which focuses on the damping torque of generator rotor movement and has a clear physical meaning [17, 18]. Authors in [19] and [20] conduct eigen-analysis to evaluate the damping impact of VSC-HVDC on sub-synchronous resonance (SSR) and design damping controller to damping SSR. Ref. [21] proposes a supplementary control scheme to improve the damping performance of the entire hybrid AC/MTDC power grid. But it only establishes the model of two-terminal AC network and thus cannot be applied to VSC-MTDC. Furthermore, these references cannot analyze the detailed damping torque mechanism for the lack of DTI analysis.

DTA analysis has been applied to quite a few new research fields and scenes for example doubly fed induction generator (DFIG) and unified power flow controller (UPFC) [22-24]. If DTA can be applied to VSC-HVDC, it will be helpful for analysis of VSC supplementary damping controller and system dynamic stability. The main innovation of this paper is to apply the classical supplementary damping controller to improve system stability and derive the DTA theory of VSC supplementary damping controller. Then it is applied to analyze the impact of damping controller on electromechanical oscillations and conduct controller designing. The main contributions of this paper are presented as follows:

- To demonstrate the mechanism of applying DTA to VSC-HVDC, this paper firstly illustrates the mechanism and transfer function of VCC and VSC supplementary damping controller and thus establishes the state-space model of power system with VSC-HVDC which lays the foundation for eigen-analysis and damping torque analysis.
- Then the DTA theory of VSC supplementary damping controller is investigated including the forward path from supplementary damping controller to electromechanical loop, signal reconstruction matrix and so on. Thus, the equation of DTI which reflects the sensitivity of the transfer function to electromechanical oscillation modes is derived.
- The index, DTI, is applied to analyze the influence of VSC supplementary damping controller on low frequency oscillations and conduct controller design. This paper presents the entire design framework based on DTI including selection of location and channel and parameter tuning and the detailed procedure of phase compensation method.

The rest of this paper is organized as follows. Section II deduces the state-space model of AC/DC hybrid system with VSC-HVDC. On this basis, Section III investigates the DTA theory of VSC supplementary damping controller and deduces the equation of DTI. Section IV presents the design framework of VSC supplementary damping controller based on DTI. Section V validates the correctness and feasibility of the proposed method in two cases. Finally, Section VI summarizes the conclusions of this paper.

II. STATE-SPACE MODEL OF VSC-HVDC AND ITS SUPPLEMENTARY DAMPING CONTROLLER

At present, there are three kinds of VSC stations in engineering applications including two-level converter, diode-clamped three-level converter and modular multilevel converter (MMC) [25]. This paper takes two-level converter for example to illustrate the linearized model of VSC. VSC station consists of AC side line, PLL, controls, PWM and gate driver and the illustrative diagram is presented in Fig. 1.

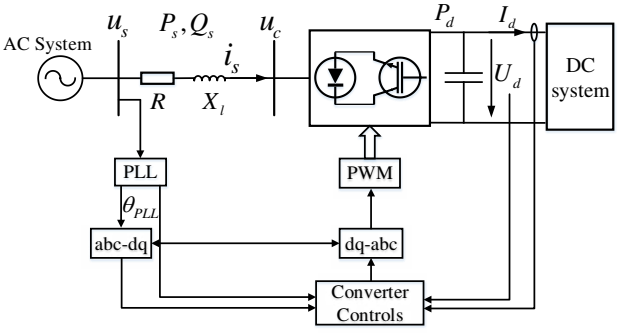

FIGURE 1. Constitutions of VSC station.

where u_s is the bus voltage connected to VSC and u_c is the AC side voltage. U_d, I_d and P_d are DC side voltage, current and power. R, X_l are the aggregated resistance and inductance of the converter transformer and phase rector considering transmission and commutation loss. $P_s + jQ_s$ is the transmission power from AC system to VSC, i_s is the

This article has been accepted for publication in a future issue of this journal, but has not been fully edited. Content may change prior to final publication. Citation information: DOI 10.1109/ACCESS.2020.3036495, IEEE Access

line current. The displayed direction of transmission is the prescriptive positive direction in this paper which means AC system transmits power to VSC station and the operation status of VSC is converter. If the transmission power is opposite to the positive direction, the operation status is inverter.

VSC stations generally adopt the current vector control with an inner-outer loop structure to conduct separate controls of active and reactive powers [26, 27]. The inner loop is aimed to conduct current decoupled control and the outer loop to control active and reactive power and DC voltage [28]. The detailed mechanism and procedure are given in Fig. 2.

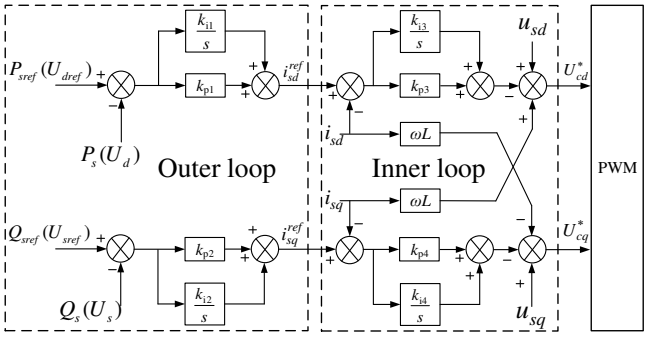

FIGURE 2. Illustrative diagram of inner-outer loop control.

where P_{sref} is the reference of the active power control and Q_{sref} are that of the reactive power control. k_{i1} to k_{i4} and k_{p1} to k_{p4} are the parameters of PI controls in the inner-outer loop control. i_{sd} and i_{sq} is the d-axis and q-axis components of i_s. Similarly, u_{sd} and u_{sq} is the components of u_s. L is the inductance corresponding to X_l, ω_0 is the original generator speed.

VSC supplementary damping controller installed in the control section can improve system damping and suppress low frequency oscillations. The output of damping controller can be provided to active or reactive power control to enhance the power control ability and improve system small-signal stability. VSC supplementary damping controller consists of three sections including amplification section, restoration section and phase compensation section. The schematic diagram is displayed in Fig. 3

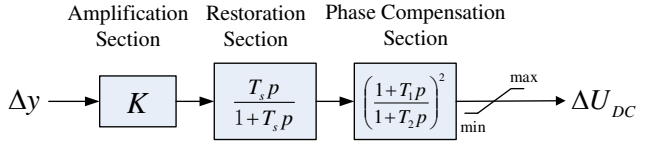

FIGURE 3. Schematic diagram of VSC supplementary damping controller. [24]

where K, T_s, T_1 and T_2 are corresponding parameters of VSC supplementary damping controller, p is the differential operator, Δy is the input signal and ΔU_{DC} is the output. The output is provided to the reference of active or reactive power.

As shown in Fig. 3, the transfer function of VSC damping controller is given as follows.

$$G_{DC}(s) = K\frac{T_p s}{1+T_p s}\left(\frac{1+T_1 s}{1+T_2 s}\right)^2 \tag{1}$$

Thus, the linearized equations of the AC/DC system with VSC and its supplementary damping controllers can be derived and presented in Equation (2) [20].

$$\begin{bmatrix}\Delta\dot{\delta}\\ \Delta\dot{\omega}\\ \Delta\dot{Z}\end{bmatrix} = \begin{bmatrix}0 & \omega_0 I & 0\\ A_{21} & A_{22} & A_{23}\\ A_{31} & A_{32} & A_{33}\end{bmatrix}\begin{bmatrix}\Delta\delta\\ \Delta\omega\\ \Delta Z\end{bmatrix} + \begin{bmatrix}0\\ B_2\\ B_3\end{bmatrix}\Delta U_{DC} \tag{2}$$

where δ is generator power angle; ω is generator speed; Z contains the other state variables of generators and the state variables of VSCs (except those of damping controllers).

The input of VSC supplementary damping controller, i.e. Δy may be selected as the deviation value of active powers or generator speeds and thus can be expressed as follows.

$$\Delta y = C\begin{bmatrix}\Delta\delta & \Delta\omega & \Delta Z\end{bmatrix}^T \tag{3}$$

where C is the coefficient matrix.

According to (1), it have

$$\Delta U_{DC} = G_{DC}(s)\Delta y \tag{4}$$

Equation (2) to (4) constitute the entire state-space model of the AC/DC system containing VSC supplementary damping controllers.

III. DAMPING TORQUE ANALYSIS OF VSC-HVDC SUPPLEMENTARY DAMPING CONTROLLER

The basic theory of damping torque analysis it to reveal the detailed mechanism of the damping torque provided by stabilizer including generation, distribution and transmission [29, 30]. According to (2), the transfer function of the path from VSC supplementary damping controller to the generator electromechanical oscillation loop can be displayed as follows.

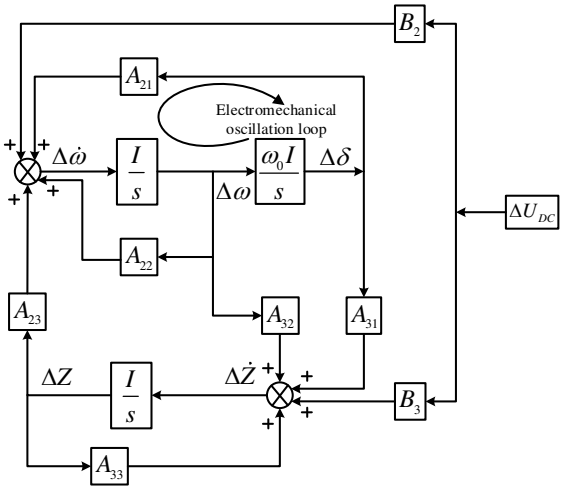

FIGURE 4. Path from VSC supplementary damping controller to the generator electromechanical oscillation loop.

This article has been accepted for publication in a future issue of this journal, but has not been fully edited. Content may change prior to final publication. Citation information: DOI 10.1109/ACCESS.2020.3036495, IEEE Access

Fig. 4 demonstrates the propagation mechanism of damping and the detailed derivation process can be found in [30]. According to Fig. 4, the forward path from VSC supplementary damping controller signal to the generator electromechanical oscillation loop can be derived in (5).

$$F(\mathrm{s}) = A_{23}(\mathrm{s}\,I - A_{33})^{-1}B_3 + B_2 \tag{5}$$

Therefore, for one electromechanical oscillation mode λ_i, the damping torque coefficient that damping controller provides to the *j*th generator electromechanical oscillation loop is derived as follows:

$$T_{Dij} = M_j[F_j(\lambda_i)\gamma_j(\lambda_i)G_{DC}(\lambda_i)] \tag{6}$$

where M_j is the inertia constant of the *j*th generator, $F_j(\lambda_i)$ is the transfer function from VSC supplementary damping controller to the *j*th generator electromechanical oscillation loop and can be calculated according to (5). $\gamma_j(\lambda_i)$ is the coefficient matrix after signal reconstruction.

According to linear control theory, the signal Δy can be reestablished through each generator speed and the equation of reconstruction matrix is presented as follows.

$$\gamma_j(\lambda_i) = \frac{\Delta y}{\Delta\omega_j} = \frac{C_{ki}V_i}{V_{i2j}} \tag{7}$$

where C_{ki} is the coefficient of reconstruction signal, V_i is part of the right eigenvector corresponding to λ_i. V_{i2j} is part of V_i corresponding to $\Delta\omega_j$ [31, 32].

The above equation reveals that VSC supplementary damping controller provides damping torque to every generator. Assume H_{ij} and φ_{ij} are respectively the amplitude and phase of the damping torque, it can be expressed as follows.

$$T_{Dij} = H_{ij}\angle\varphi_{ij} = F_j(\lambda_i)\frac{C_{ki}V_i}{V_{i2j}} \tag{8}$$

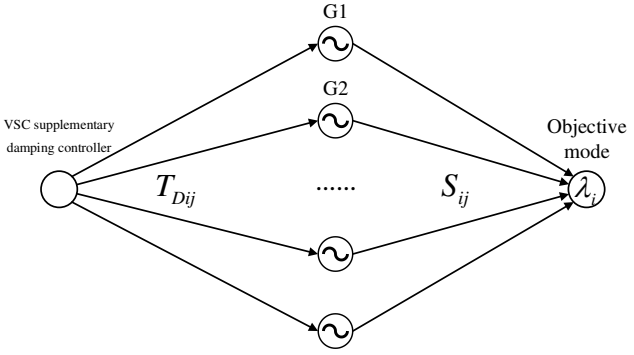

FIGURE 5. Illustrative diagram of damping transfer from VSC supplementary damping controller to objective modes.

As shown in Fig. 5, VSC supplementary damping controller influences electromechanical oscillations modes through generators, the impact every generator exerts on oscillation modes must be considered. Define S_{ij} is the sensitivity of oscillation mode to the damping torque coefficient on the *j*th generator.

$$S_{ij} = \frac{\partial\lambda_i}{\partial T_{Dij}} \tag{9}$$

Thus, the DTI of VSC supplementary damping controller is derived

$$S^i_{DTA} = \frac{\Delta\lambda_i}{\Delta G_{DC}(\lambda_i)} = \sum_{j=1}^{N} S_{ij}H_{ij}\angle\varphi_{ij} = \sum_{j=1}^{N} S_{ij}M_jF_j(\lambda_i)\frac{C_{ki}V_i}{V_{i2j}} \tag{10}$$

IV. DESIGN OF VSC-HVDC SUPPLEMENTARY DAMPING CONTROLLER BASED ON DTA

The design of VSC supplementary damping controller consists of installation location selection, channel selection and parameter tuning. One VSC station has two damping channels, i.e. active and reactive power control channels. The selection of installation location and channel can be decided according to DTI. DTI is defined to reflect the sensitivity of one electromechanical oscillation mode to the transfer function of supplementary damping controller. Therefore, the biggest amplitude of DTI means controller installed at that location or channel will exert the greatest impact on the objective mode. In conclusion, the designed damping controller should maximize its influence on modal damping. The optimization objective is given in (11).

$$\max: \left|S_{DTA}(y)\right| \tag{11}$$

where y is the different controller condition including installation location, channel, feedback signal and controller parameters. DTI represents the impact ability of damping controller on objective mode. Thus, the criterion of controller designing is to get the maximal DTI.

After selection of installation location and channel, controller parameter tuning can be conducted by phase compensation method. The design framework of VSC supplementary damping controller is displayed in Fig. 6.

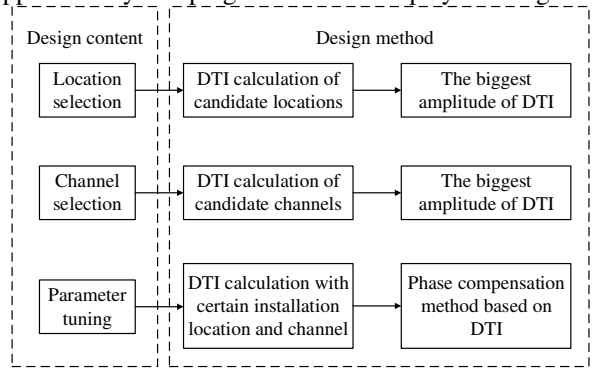

FIGURE 6. Design framework of VSC supplementary damping controller based on DTI.

The mechanism of phase compensation method is as follows: according to the definition of DTI, the change of the *i*th mode caused by VSC supplementary damping controller is shown in (12).

This article has been accepted for publication in a future issue of this journal, but has not been fully edited. Content may change prior to final publication. Citation information: DOI 10.1109/ACCESS.2020.3036495, IEEE Access

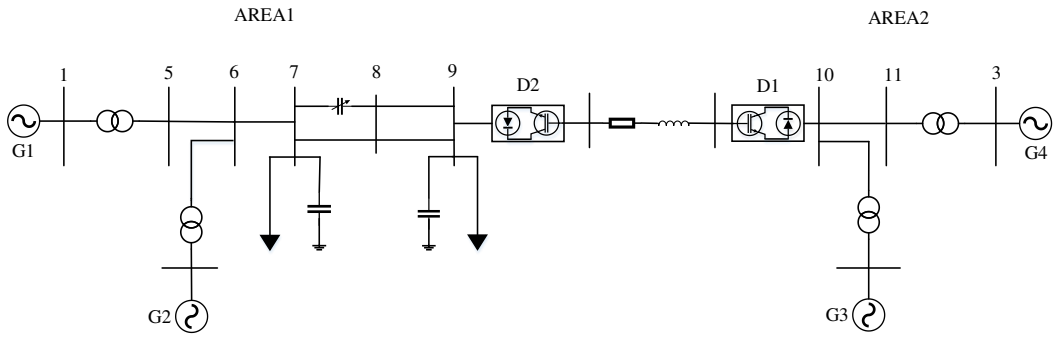

FIGURE 8. **Network of Case A.**

$$\Delta\lambda_i = S^i_{DTA}\Delta G_{DC}(\lambda_i) \tag{12}$$

As shown in Fig. 7, the objective of phase compensation method is to shift the *i*th mode horizontally to the left side [33, 34]. It is the most efficient way to damp the objective mode with the frequency constant. Thus, the compensation phase caused by VSC supplementary damping controller should be

$$angle(G_{DC}(\lambda_i)) = 180^\circ - angle(S^i_{DTA}) \tag{13}$$

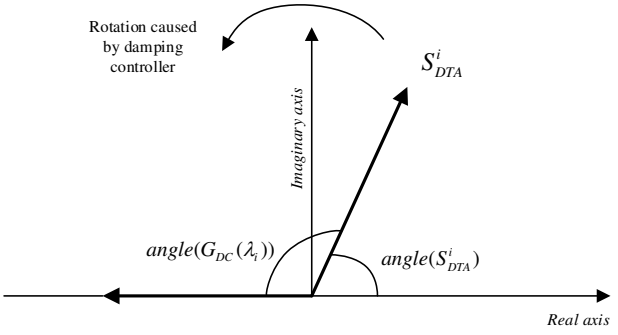

FIGURE 7. **Design mechanism of phase compensation method.**

The phase adjusting of VSC supplementary damping controller mainly depends on the phase compensation section, especially T_1 . T_2 and T_s are usually decided according to experience and K can be decided according to the expected damping torque. The value of T_1 need to be tuned by phase compensation method.

V. CASE STUDY

A. CASE A

Firstly, simulations are conducted in Case A (Fig. 8) to verify the proposed design method. Two-area four-machine (2A4M) system is a classical system for small-signal stability analysis with one inter-area mode and two inner-area modes. In Case A, a two-terminal VSC system is used to interconnect two areas to substitute the primary AC transmission line. The detailed parameters of this system are available in [35]. Compared to the original 2A4M system, a series compensation and two capacitors are added to adjust power flow and improve system stability. The line impedance between Bus 7 and 8 with the series compensation is 0.011 + j0.11 p.u.. The susceptance of capacitors in Bus 7 and 9 are 2.0 and 3.5 p.u. respectively. Master-slave control is adopted and the detailed control parameters are given in Tab. 1.

TABLE 1. **Control modes and parameters of Case A.**

VSC station	Control mode	Active power control/p.u.	Reactive power control/p.u.
D1	Master	$U_d = 2.0$	$Q_s = 1.299$
D2	Slave	$P_s = -2.0$	$\lvert U_s\rvert = 1.0$

Conduct linearization to Case A, the eigen-analysis results are presented in Tab. 2.

TABLE 2. **Eigen-analysis results of Case A.**

Mode	Eigenvalue	Frequency/Hz	Damping ratio
Mode 1	0.2084 + j4.8459	0.7712	-4.30%
Mode 2	0.04283 + j4.3311	0.6893	-0.989%

The original 2A4M system is a poorly damped system with three electromechanical oscillation modes. Tab. 2 shows there are only two oscillation modes in Case A. According to the results of participation factors, Mode 1 is the inner-area mode of Area 1 and Mode 2 is that of Area 2. Therefore, the inter-area mode is eliminated by DC system. This reflects the isolation effect of VSC system on inter-area modes.

TABLE 3. **DTI calculation results of Case A.**

Location	Channel	S^1_{DTA}	$\lvert S^1_{DTA}\rvert$	S^2_{DTA}	$\lvert S^2_{DTA}\rvert$
D1	Active power	-0.00455 + j0.0250	0.0254	1.52×10^{-4} - $j7.04\times10^{-5}$	1.68×10^{-4}
	Reactive power	0.00224 - j0.0187	0.0188	8.27×10^{-5} - $j1.11\times10^{-5}$	8.34×10^{-5}
D2	Active power	1.84×10^{-5} + $j2.19\times10^{-4}$	2.20×10^{-4}	0.00479 - j0.0132	0.0140
	Reactive power	-2.29×10^{-6} + $j2.29\times10^{-7}$	2.32×10^{-6}	0.00372 - j0.000386	0.00374

Assume the input signal of supplementary damping controller installed at D1 is $\Delta\omega_3 - \Delta\omega_4$ and that of D2 is $\Delta\omega_1 - \Delta\omega_2$, where $\Delta\omega_i$ is the deviation value of the *i*th

This article has been accepted for publication in a future issue of this journal, but has not been fully edited. Content may change prior to final publication. Citation information: DOI 10.1109/ACCESS.2020.3036495, IEEE Access

generator speed. Conduct DTI calculations with different installation locations and channels, the results are presented in Tab. 3. In this table, S^1_{DTA} is the DTI of Mode 1 and $\left|S^1_{DTA}\right|$ is the amplitude. S^2_{DTA} and $\left|S^2_{DTA}\right|$ are those of Mode 2.

From the above table, it is revealed that VSC supplementary damping controller installed at D1 exerts a much greater impact than D2 on Mode 1, the inner-area mode of Area 1. Similarly, damping controller installed at D2 has a greater influence on Mode 2. Therefore, it can be drawn that VSC-HVDC system equivalently separate the AC system and VSC supplementary damping controller can damp the inner-area oscillation mode of the same area but has a very weak influence on the modes of the other areas. In addition, Tab. 3 also shows the active power channel has a damping effect than the reactive power channel.

K is assigned to be 10 according to the requirement of damping torque. Then conduct VSC supplementary damping controller parameter tuning using phase compensation method with different locations and channels and the results are shown in Tab. 4.

TABLE 4. VSC supplementary damping controller parameter tuning results of Case A.

Location	Channel	T_1
D1	Active power	0.2522
	Reactive power	0.1517
D2	Active power	0.3658
	Reactive power	0.2326

Install supplementary damping controller at the active power channel of D1 with the tuned parameter. Assume a three-phase short-circuit fault happens at bus B8 at 0.1s and then is cleared 0.01 s later. Simulations are conducted with and without damping controller and the comparative curves are displayed in Fig. 9.

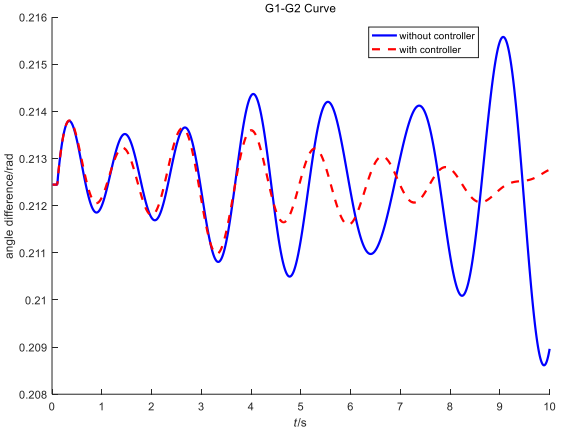

(a)

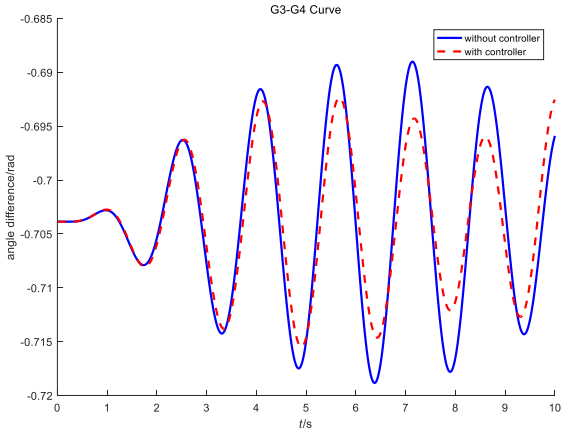

(b)

FIGURE 9. Comparative simulation curves with and without VSC supplementary damping controller at D1.

Fig. 9 shows VSC supplementary damping controller installed at D1 can effectively inhibit oscillations in Area 1 but has a weak influence on oscillations in Area 2. This is in consistence with the DTI results and demonstrates the feasibility of the proposed method of this paper. To reveal the damping effect in Fig. (b) more clearly, Prony analysis is conducted and the results are shown in Tab. 5.

TABLE 5. Prony analysis results of curves in Fig. 9 (b).

	Amplitude	Phase	Frequency	Attenuation coefficient
Without controller	0.007353	3.039	0.6893	0.04283
With controller	0.006946	3.272	0.6804	0.05769

Tab. 5 presents the Prony analysis results of major oscillation mode in Fig. 9 (b). As shown in the table, the attenuation coefficient with damping controller is better than without controller. But the effect is not very distinct which is consistent with DTI results.

Then supplementary damping controller is installed at active and reactive power channel of D1 and the simulation results are presented below.

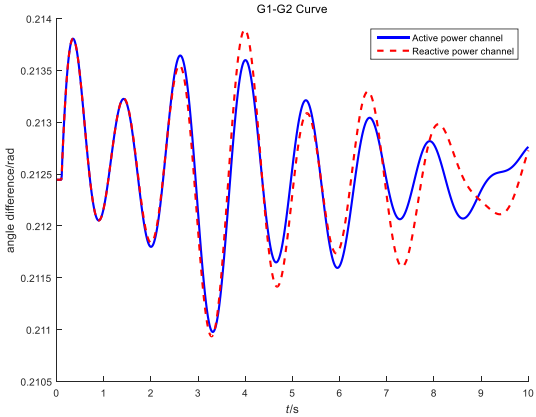

FIGURE 10. Comparative simulation curves of different channels.

This article has been accepted for publication in a future issue of this journal, but has not been fully edited. Content may change prior to final publication. Citation information: DOI 10.1109/ACCESS.2020.3036495, IEEE Access

As shown in Fig. 10, VSC supplementary damping controller installed at the active power channel has a better damping effect than the reactive channel which also demonstrates the correctness of DTI calculation results.

To improve the small-signal stability of the whole AC/DC system, VSC supplementary damping controllers are installed at the active power channels of D1 and D2 simultaneously with the tuned parameters. According to DTI calculation results, the damping torque contribution and its transmission procedure provided by damping controllers to oscillation modes are presented in Fig. 11.

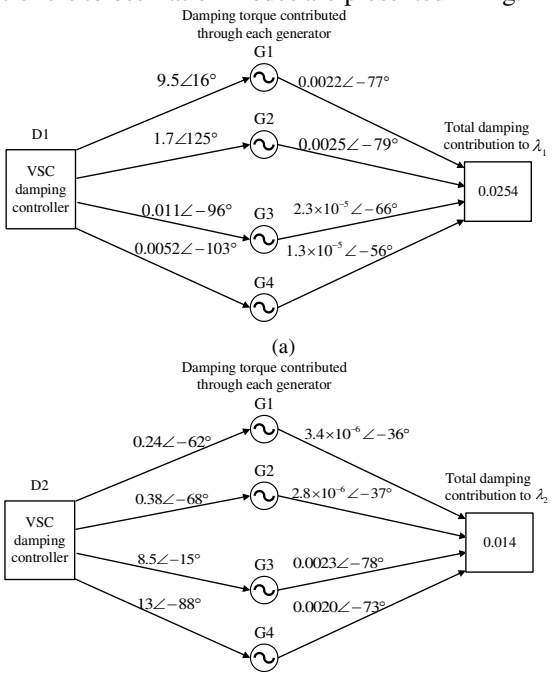

FIGURE 11. Damping torque contribution and transmission of VSC supplementary damping controllers.

Conduct eigen calculation and simulations to systems with and without VSC damping controllers, the modal trajectories are shown in Fig. 12. Comparative simulation curves are given in Fig. 13.

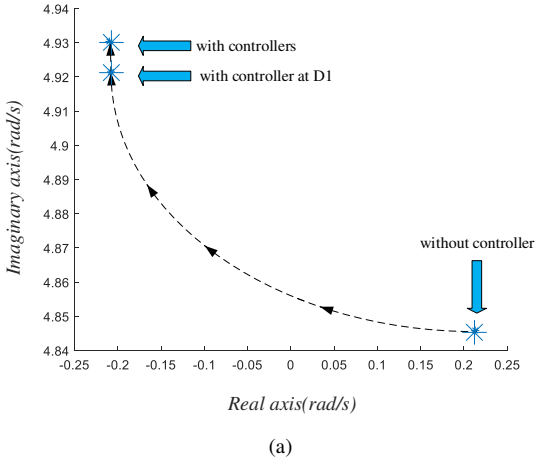

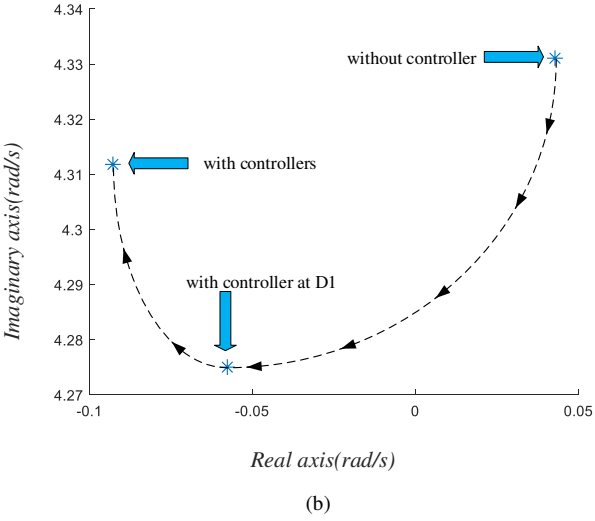

FIGURE 12. Modal trajectories with and without damping controllers.

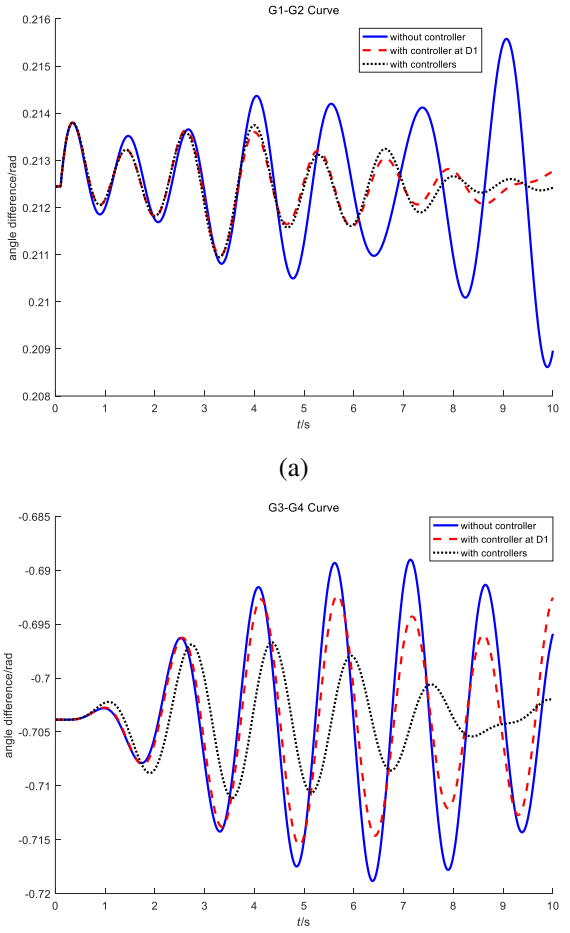

This article has been accepted for publication in a future issue of this journal, but has not been fully edited. Content may change prior to final publication. Citation information: DOI 10.1109/ACCESS.2020.3036495, IEEE Access

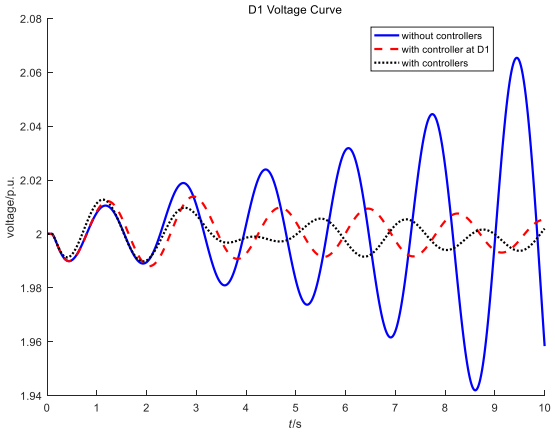

(c)

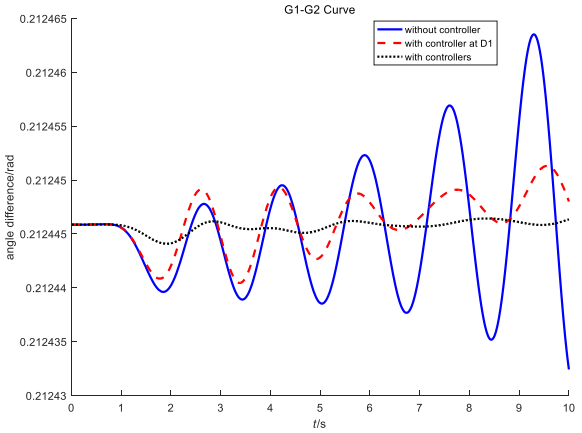

(a)

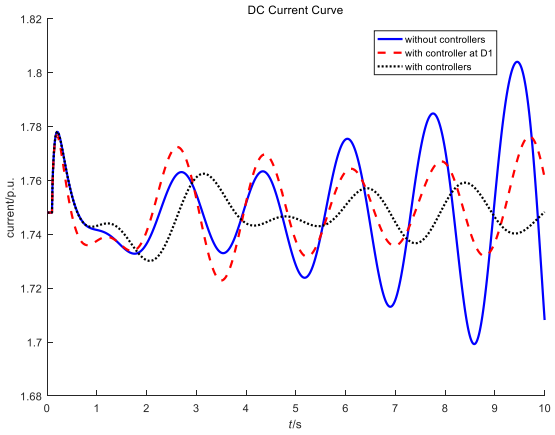

(d)

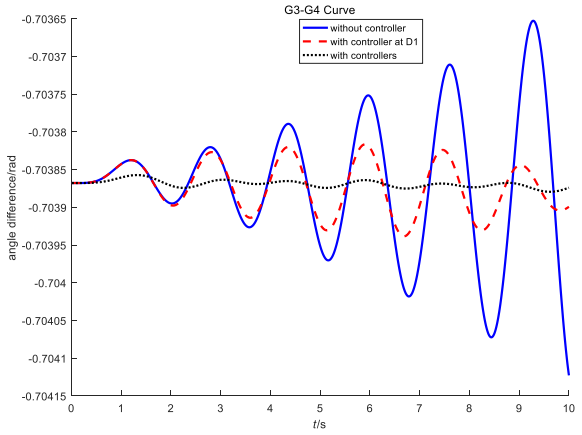

(b)

FIGURE 13. **Comparative simulation curves under different conditions.**

FIGURE 14. **Comparative simulation curves after DC power modulation.**

The modal trajectories and simulation curves in Fig. 12 and Fig. 13are consistent with DTI results. The damping controllers at two areas have excellent performances to suppress oscillations in both areas. This demonstrates damping controllers at different areas can be designed separately as the interactions between areas are relatively very weak. In addition, the damping effect of VSC supplementary damping controllers is better than single controller at D1. This reflects the power controls of both VSC station are enhanced by VSC supplementary damping controllers so as to improve the overall damping effect and stability.

In order to demonstrate the damping effect of different small disturbances, the active power of D1 is modulated to 2.1 p.u. at 0.1s, simulation curves are shown in Fig. 14.

According to Fig. 14, the small disturbance in DC system can transfer oscillations to AC systems and other areas. The simulation curves show different oscillation performances with faults in AC system. In addition, due to the modulation of VSC station power, the oscillation curves have a deviation to the original stable operation point.

B. CASE B

To verify the proposed method in a large-scale system with VSC-MTDC, Case B (Fig. 15) is applied to interconnect two nonsynchronous power systems with a four-terminal VSC system. The information and parameters of the two systems are available in [36, 37] including NYPS (New York Power System) and NETS (New England Test System). The detailed parameters are given in [38] and Tab. 6.

TABLE 6. **Control modes and parameters of Case B.**

VSC station	Operation mode	Control mode	Active power control/p.u.	Reactive power control/p.u.
D1	Inverter	Master	$U_d = 2.0$	$Q_s = -0.2$
D2	Inverter	Slave	$P_s = -0.5$	$\|U_s\| = 1.0$
D3	Rectifier	Slave	$P_s = 0.5$	$Q_s = 0.3$
D4	Rectifier	Slave	$P_s = 0.5$	$Q_s = 0.3$

According to DTI analysis results, VSC supplementary damping controllers are installed at the active power channels of D1 and D4 with the tuned parameters. K is assigned to be 20. A small signal is applied to B47 in NYPS

This article has been accepted for publication in a future issue of this journal, but has not been fully edited. Content may change prior to final publication. Citation information: DOI 10.1109/ACCESS.2020.3036495, IEEE Access

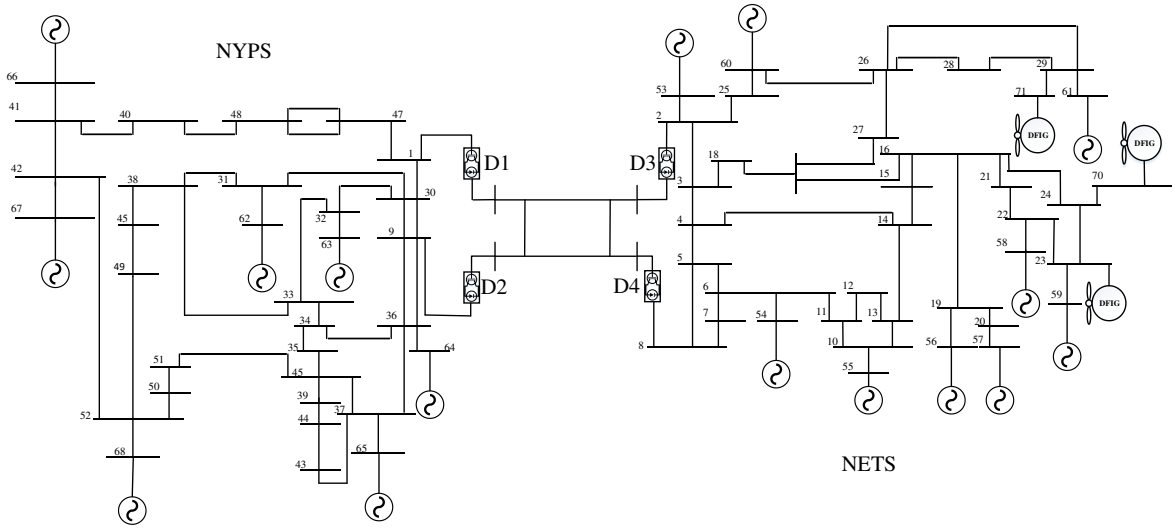

FIGURE 15. Network of Case B.

at 0.1s and cleared 0.01s later. The simulation results are displayed in Fig. 16.

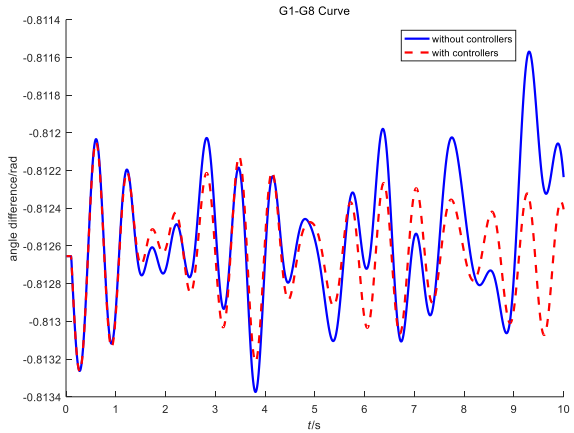

(a)

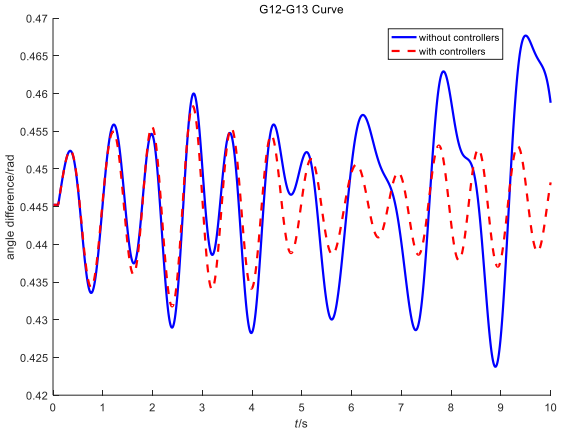

(b)

FIGURE 16. Comparative simulation curves of Case B with and without VSC supplementary damping controllers.

where G1 and G8 are generators of NETS and G12 and G13 are those of NYPS. The two diagrams respectively reflect oscillation behaviors in two power grids.

The simulation curves show the oscillation curves in Fig. 16 are more complex than Case A. Besides, it is also revealed the power angle difference between different areas has lost synchronization after the fault and the interactions are very weak for the separation of DC system. Therefore, for large-scale nonsynchronous power grids connected by VSC-HVDC, VSC supplementary damping controllers should be installed in respective areas to damp oscillations and enhance the dynamic stability of the whole AC/DC system.

VI. CONCLUSION

The major contribution of this paper is to extend the damping torque analysis theory to supplementary damping control of VSC-HVDC to inhibit oscillations in AC/DC hybrid system. DTA is applied to investigate the influence mechanism of VSC-HVDC and guide the design of VSC supplementary damping controller including location and channel selection and parameter tuning. The simulation results and analysis show that the proposed method can reveal the oscillation mechanism in AC/DC hybrid system and guide controller designing to suppress oscillations. Some conclusions from the damping torque analysis and time-domain simulations are drawn as follows:

(1) VSC-HVDC has a great impact on the dynamic stability of AC/DC system including oscillation performance and eigen-analysis results. VSC-HVDC equivalently divides the whole power system into several independent areas. The interactions between areas for low frequency oscillation are very weak. Therefore, the most important

factors to threaten the small-signal stability of the AC/DC system are inner-area modes.

(2) Oscillations associated with a single generator or generators in one area are called inner-area oscillations. Each area has its own inner-area oscillation mode. VSC supplementary damping controller can effectively inhibit the inner-area modes of but exerts a very weak impact on oscillations of other areas. Therefore, for a large-scale AC/DC system, VSC supplementary damping controllers should be installed in respective areas to damp inner-area oscillations so as to improve the small-signal stability of the whole system.

(3) In traditional analysis of low frequency oscillations, damping controllers generally adopt power angles and speeds to suppress low frequency oscillations. On the other hand, variables of VSC stations also strongly couple with generator angles and speeds. For example, generator speed has a non-negligible impact on the internal frequency of VSC station. The damping effect and mechanism of VSC damping controllers adopting VSC variables are of great research value and will be our next research direction.

(4) In this paper, VSC supplementary damping controller is designed to be installed at the optimal location and channel to damp oscillations. However, one oscillation mode may be impacted by several generators and supplementary damping controllers. As shown in Case B, the damping effect is not very ideal in some large-scale complex power systems. Therefore, the coordinated design and optimization of multiple locations and channels and with power system stabilizer (PSS) will be our research direction of next stage.

REFERENCES

[1] W. Wang, Y. Li, Y. Cao, U. Hager, and C. Rehtanz, "Adaptive droop control of VSC-MTDC system for frequency support and power sharing," *IEEE Trans. Power Syst*., vol. 33, no. 2, pp. 1264–1274, Mar. 2018.

[2] G. Wu, Z. Du, C. Li, and G. Li, "VSC-MTDC operation adjustments for damping inter-area oscillations," *IEEE Trans. Power Syst*., vol. 1, no. 1, pp. 1373–1382, Mar. 2018.

[3] A. Raza et al., "A protection scheme for multi-terminal VSC-HVDC transmission systems," *IEEE Access*, vol. 6, pp. 3159–3166, 2018.

[4] M. F. M. Arani and Y. A. R. I. Mohamed, "Analysis and performance enhancement of vector-controlled VSC in HVDC links connected to very weak grids," *IEEE Trans. Power Syst*., vol. 32, no. 1, pp. 684–693, Jan. 2017.

[5] J. Z. Zhou, H. Ding, S. Fan, Y. Zhang, and A. M. Gole, "Impact of short-circuit ratio and phase-locked-loop parameters on the small-signal behavior of a VSC-HVDC converter," *IEEE Trans. Power Deliv*., vol. 29, no. 5, pp. 2287–2296, Oct. 2014.

[6] X. Bian, Y. Ding, K. Mai, Q. Zhou, Y. Zhao, and L. Tang, "Subsynchronous oscillation caused by grid-connection of offshore wind farm through VSC-HVDC and its mitigation," *Autom. Electr. Power Syst*., vol. 42, no. 17, pp. 25–33, 2018.

[7] W. Du, Q. Fu, and H. Wang, "Subsynchronous oscillations caused by open-loop modal coupling between VSC-based HVDC line and power system," *IEEE Trans. Power Syst*., vol. 33, no. 4, pp. 3664–3677, Jul. 2018.

[8] W. Du, Q. Fu, and H. Wang, "Method of open-loop modal analysis for examining the subsynchronous interactions introduced by VSC control in an MTDC/AC system," *IEEE Trans. Power Deliv*., vol. 29, no. 5, pp. 2287–2296, Apr. 2018.

[9] R. Preece, J. V. Milanović, A. M. Almutairi, and O. Marjanovic, "Damping of inter-area oscillations in mixed AC/DC networks using WAMS based supplementary controller," *IEEE Trans. Power Syst*., vol. 28, no. 2, pp. 1160–1169, May. 2013,.

[10] Z. Yao, Q. Zhang, P. Chen, and Q. Zhao, "Research on fault diagnosis for MMC-HVDC systems," *Prot. Control Mod. Power Syst*., vol. 1, no. 1, pp. 1–7, 2016.

[11] Y. Zhang, K. Liu, X. Li, and L. Zhang, "Design of decentralized robust damping controller for VSC-HVDC transmission system based on homotopic transformation," *Proc. CSEE*, no. 8, pp. 25–33, 2016.

[12] R. Preece and J. V. Milanovic, "Tuning of a damping controller for multiterminal VSC-HVDC grids using the probabilistic collocation method," *IEEE Trans. Power Deliv*., vol. 29, no. 1, pp. 318–326, Feb. 2014.

[13] B. Ni, W. Xiang, X. Lu, and J. Wen, "Low-frequency oscillation suppression using flexible DC grid based on state feedback supplementary damping control," *Electr. Power Autom. Equip*., no. 3, pp. 45–50, 2019.

[14] R. Preece, J. V. Milanović, A. M. Almutairi, and O. Marjanovic, "Probabilistic evaluation of damping controller in networks with multiple VSC-HVDC lines," *IEEE Trans. Power Syst*., vol. 28, no. 1, pp. 367–376, Feb. 2013.

[15] A. Fuchs, M. Imhof, T. Demiray, and M. Morari, "Stabilization of large power systems using vsc-hvdc and model predictive control," *IEEE Trans. Power Deliv*., vol. 29, no. 1, pp. 480–488, Feb. 2014.

[16] L. Huang, H. Xin, and Z. Wang, "Damping low-frequency oscillations through VSC-HVdc stations operated as virtual synchronous machines," *IEEE Trans. Power Electron*., vol. 34, no. 6, pp. 5803–5818, Jun. 2019.

[17] H. F. Li, W. Du, H. F. Wang, and L. Y. Xiao, "Damping torque analysis of energy storage system control in a multi-machine power system," *IEEE PES Innovative Smart Grid Technologies Conference Europe*, Dec. 2011.

[18] F. J. Swift and H. Wang, "The connection between modal analysis and electric torque analysis in studying the oscillation stability of multi-machine power systems," *Int. J. Electr. Power Energy Syst*., vol. 15, no. 5, pp. 321–330, 1997.

[19] T. Joseph, C. Ugalde-Loo, S. Balasubramaniam, and J. Liang, "Real-Time Estimation and Damping of SSR in a VSC-HVDC Connected Series-Compensated System," *IEEE Trans. Power Syst*., vol. 33, no. 6, pp. 7052 - 7063, Nov. 2018.

[20] N. Prabhu and K. R. Padiyar, "Investigation of Subsynchronous Resonance With VSC-Based HVDC Transmission Systems," *IEEE Trans. Power Deliv*., vol. 24, no. 1, pp. 433–440, Jan. 2009.

[21] M. Gu, L. Meegahapola and K. L. Wong, "Damping Performance Analysis and Control of Hybrid AC/Multi-Terminal DC Power Grids," *IEEE Access*, vol. 7, pp. 118712-118726, 2019.

[22] W. Du, J. Bi, J. Cao, and H. Wang, "A method to examine the impact of grid connection of the DFIGs on power system electromechanical oscillation modes," *IEEE Trans. Power Syst*., vol. 31, no. 5, pp. 3775–3784, Sept. 2016.

[23] B. Ren, W. Du, and H. Wang, "Damping torque analysis of electromechanical oscillation modes for power system affected by grid-connected UPFC," *Autom. Electr. Power Syst*., vol. 42, no. 17, pp. 18–30, 2018.

[24] B. Ren, W. Du, and H. Wang, "Damping channel selection based on damping torque analysis and coordinated design of auxiliary stabilizer for UPFC," *Electr. Power Autom. Equip*., vol. 37, no. 5, pp. 18–24, 2017.

[25] R. Chai, B. Zhang, and Z. Bo, "Alternating iterative power flow algorithm for hybrid AC/DC networks containing DC grid based on voltage source converter," *Autom. Electr. Power Syst*., vol. 39, no. 7, pp. 7–13, 2015.

[26] N. R. Chaudhuri, R. Majumder, B. Chaudhuri, and J. Pan, "Stability analysis of VSC MTDC grids connected to multimachine AC

systems," *IEEE Trans. Power Deliv*., vol. 26, no. 4, pp. 2774–2784, Oct. 2011.

[27] S. Cole, J. Beerten, and R. Belmans, "Generalized dynamic VSC MTDC model for power system stability studies," *IEEE Trans. Power Syst*., vol. 25, no. 3, pp. 1655–1662, Aug. 2010.

[28] B. Parkhideh and S. Bhattacharya, "Vector-controlled voltage-source-converter-based transmission under grid disturbances," *IEEE Trans. Power Electron*., vol. 28, no. 2, pp. 661–672, Feb. 2013.

[29] W. Du, J. Bi, C. Lv, and T. Littler, "Damping torque analysis of power systems with DFIGs for wind power generation," *IET Renewable Power Generation*, vol. 11, no. 1, pp. 10–19, Apr. 2017.

[30] T. Zhou, Z. Chen, R. Zhou. "Power system stabilizer parameter tuning based on closed-loop damping torque analysis method," *Autom. Electr. Power Syst*. 2016, vol. 40, no. 18, pp. 56–60.

[31] Z. Chen, W. Du, H. Wang, S. Gao. "Power system low-frequency oscillation suppression with energy storage system based on DTA," *Autom. Electr. Power Syst*. 2009, vol. 33, no. 12, pp. 8–11.

[32] Z. Chen. "Study of the DTA application in large scale inter-connected power system," *Power Syst. Prot. Control* 2011, vol. 39, no. 12, pp. 102–105.

[33] J. Zhang, C. Y. Chung, and Y. Han, "A novel modal decomposition control and its application to PSS design for damping interarea oscillations in power systems," *IEEE Trans. Power Syst*., vol. 27, no. 4, pp. 2015–2025, Nov. 2012.

[34] T. Zhou, Z. Chen, S. Bu, H. Tang, and Y. Liu, "Eigen-analysis considering time-delay and data-loss of WAMS and its application to WADC design based on damping torque analysis," *Energies*, vol. 11, no. 11, pp. 3186, 2018.

[35] M. Klein, G. J. Rogers, and P. Kundur, "A fundamental study of inter-area oscillations in power systems," *IEEE Trans. Power Syst.*, Aug. 1991.

[36] G. Rogers, Power System Oscillations. Norwell, MA, USA: Kluwer, 2000.

[37] S. Q. Bu, W. Du, H. F. Wang, Y. Liu, and X. Liu, "Investigation on economic and reliable operation of meshed MTDC/AC grid as impacted by offshore wind farms," *IEEE Trans. Power Syst.*, vol. 32, no. 5, pp. 3901–3911, Sept. 2017.

[38] H. Akagi and H. Sato, "Control and performance of a doubly-fed induction machine intended for a flywheel energy storage system," *IEEE Trans. Power Electron*., vol. 17, no. 1, pp. 109–116, Jan. 2002.